Dimer Dissociation and Thermosensitivity Kinetics of the *Saccharomyces cerevisiae* and Human TATA Binding Proteins†

Amy J. Jackson-Fisher,‡,§ Sandeep Burma,‡,|| Matthew Portnoy,‡,⊥ Lumelle A. Schneeweis,‡,# Robert A. Coleman,‡,▽ Madhusmita Mitra, Carmelata Chitikila, and B. Franklin Pugh*

Center for Gene Regulation, Department of Biochemistry and Molecular Biology, The Pennsylvania State University, University Park, Pennsylvania 16803

Received April 21, 1999; Revised Manuscript Received June 2, 1999

ABSTRACT: A kinetic analysis of dimer dissociation, TATA DNA binding, and thermal inactivation of the yeast *Saccharomyces cerevisiae* and human TATA binding proteins (TBP) was conducted. We find that yeast TBP dimers, like human TBP dimers, are slow to dissociate in vitro ($t_{1/2}$ ∼20 min). Mild mutations in the crystallographic dimer interface accelerate the rate of dimer dissociation, whereas severe mutations prevent dimerization. In the presence of excess TATA DNA, which measures the entire active TBP population, dimer dissociation represents the rate-limiting step in DNA binding. These findings provide a biochemical extension to genetic studies demonstrating that TBP dimerization prevents unregulated gene expression in yeast [Jackson-Fisher, A. J., Chitikila, C., Mitra, M., and Pugh, B. F. (1999) *Mol. Cell 3*, 717−727]. In the presence of vast excesses of TBP over TATA DNA, which measures only a very small fraction of the total TBP, the monomer population in a monomer/dimer equilibrium binds DNA rapidly, which is consistent with a simultaneous binding and bending of the DNA. Under conditions where other studies failed to detect dimers, yeast TBP's DNA binding activity was extremely labile in the absence of TATA DNA, even at temperatures as low as 0 °C. Kinetic analyses of TBP instability in the absence of DNA at 30 °C revealed that even under fairly stabilizing solution conditions, TBP's DNA binding activity rapidly dissipated with $t_{1/2}$ values ranging from 6 to 26 min. TBP's stability appeared to vary with the square root of the TBP concentration, suggesting that TBP dimerization helps prevent TBP inactivation.

The TATA binding protein (TBP)[1] plays a central role in gene expression from eucarya to archaea (*1*). Through interactions with the TATA box promoter element, located approximately 30 nucleotides upstream of the transcriptional start site, TBP nucleates the assembly of the transcription machinery. In vivo, TBP is blocked from accessing promoter DNA of uninduced genes, making its recruitment a key rate-limiting step in gene expression. Activators and coactivators function in part to facilitate TBP/TATA binding, thereby accelerating this step.

The intrinsic affinity of TBP monomers for TATA DNA is sufficiently high and its kinetics sufficiently fast that TBP/TATA interactions cannot adequately account for the intrinsic inefficiency of promoter binding in vivo. In principle, repression of the promoter and/or TBP could prevent TBP from binding TATA. For at least some uninduced genes in yeast cells, auto-repression of TBP through dimerization has recently been demonstrated to be responsible for preventing unregulated gene expression (*2*).

TBP is a saddle-shaped protein whose concave surface makes largely hydrophobic and van der Waals interactions with the minor groove of DNA (*3*). In the absence of DNA, the conserved core of TBP crystallized as a dimer, in which the C-terminal stirrups interlocked and occluded its DNA binding surface (*4*). Recent mutagenesis of the yeast TBP (yTBP) crystallographic dimer interface indicates that the crystal structure faithfully represents the structure of yTBP dimers in solution and in vivo (*2*). In vitro kinetic analyses of dimer dissociation and DNA binding with human TBP (hTBP) indicate that dimer dissociation is a rate-limiting step in DNA binding (*5*). Yeast and mouse TBP have also been reported to self-associate into dimers and other higher order structures at nanomolar concentrations in the absence of DNA (*6*, *7*).

A variety of kinetic and thermodynamic studies have not detected yTBP dimers in solution (*8*−*11*). The basis for this is unclear, but might be due to differences in methods of analysis and/or solution conditions. TBP/DNA association kinetics have generally been performed in the presence of

† This work was supported by grants from the National Institutes of Health (GM47855) and the American Cancer Society. B.F.P. is a Scholar of the Leukemia Society of America.

* To whom correspondence should be addressed. E-mail: bfp2@psu.edu.

‡ These authors contributed equally to this work.

§ Current address: Department of Pathology, Yale School of Medicine, New Haven, CT 06510.

|| Current address: Life Sciences Division, Lawrence Berkeley National Laboratory, Berkeley, CA 94720.

⊥ Current address: Department of Biochemistry, Johns Hopkins University, Baltimore, MD 21218.

Current address: SmithKline Beecham Pharmaceuticals, King of Prussia, PA 19406.

▽ Current address: ETH−Honggerberg, Institut fur Molekularbiologie und Biophysik, Zurich, Switzerland.

[1] Abbreviations: yTBP, yeast TATA binding protein; hTBP, human TBP; GST-180C, glutathione-*S*-transferase fused to the conserved 180 carboxyl-terminal amino acids of TBP; BMH, bis(maleimido)hexane.

10.1021/bi990911p CCC: $18.00
Published on Web 08/12/1999

vast molar excesses of TBP over TATA DNA. This type of analysis is valid if TBP is conformationally homogeneous. However, if TBP resides in multiple conformational and/or oligomeric states, only the binding of the fastest subpopulation will be observed. This subpopulation might represent a small fraction of the total protein. A nonlinear relationship between k_{obs} (observed pseudo-first-order rate constant of TBP/TATA binding) and [TBP] would signify multiple linked equilibria. However, an apparent linear relationship between k_{obs} and [TBP], while suggestive of a simple second-order reaction, does not exclude the possibility of more complex behavior. Within experimental uncertainty, multiple linked equilibria may give the appearance of linearity.

Protein−protein and protein−DNA interactions often involve large net changes in bound water and ions, and thus can be very sensitive to solution conditions. TBP dimerization studies have largely been performed under solution conditions that are optimal for in vitro transcription. Other TBP−DNA and TBP self-association studies have employed simpler solution conditions that may be more suitable for the assay employed (*9*, *11*). It is possible that one set of solution conditions favors dimerization/oligomerization while another set does not.

TBP has been reported to be thermosensitive, where its transcriptional activity is destroyed by a 15 min incubation at 47 °C under in vitro transcription conditions (*12*). However, its activity is very thermostable when bound to DNA (*13*). A number of previous studies on TBP/TATA association and TBP self-association involved prolonged preincubations of yTBP at 30 °C in the absence of DNA (*9*, *11*). What effect such preincubations had on TBP's DNA binding activity was not determined. DNA binding kinetics and self-association reactions are further complicated if conditions are employed where TBP monomers and dimers/oligomers have different thermostabilities.

The focus of this paper is to provide additional details on the stability of the dimer interface of yeast and human TBP, and to address the apparent discrepancy between studies that detect self-association and those that do not. First, we provide evidence that yTBP self-associates at nanomolar concentrations. Second, we show that dissociation of yTBP dimers/oligomers through the crystallographic dimer interface is slow and overall rate-limiting in TATA DNA binding. Mutations in the dimer interface are used to demonstrate the specificity of the kinetic reaction for dimer dissociation, as well as measure the relative contribution of specific side chains to dimer stability. Third, we show that under conditions (30 °C, no glycerol or detergent) previously used to examine TBP−DNA binding and self-association (*9*, *11*), TBP's DNA binding activity is rapidly inactivated when not bound to DNA. Inactivation studies with hTBP suggest that TBP self-association helps stabilize TBP from inactivation. From these studies, we conclude that yTBP dimerizes at nanomolar concentrations in vitro according to its crystallographic structure. Additional higher order structures, such as dimers of dimers, that are not detectable in our assays may also exist. In addition, our findings indicate that kinetic and thermodynamic analyses on TBP performed in standard Tris, KCl, $MgCl_2$ buffer at physiological temperatures are complicated by a variety offsetting linked equilibria that may produce an impression of a simple homogeneous active monomeric state.

MATERIALS AND METHODS

Reactions. All proteins and DNA were purified and quantified as described (*2*, *14*). The TATA DNA corresponds to a double-stranded 28 bp synthetic adenovirus major late TATA sequence; the mutant version was TAAG instead of TATA. Unless otherwise noted, all reactions contained 20 mM Tris−acetate, pH 7.5, 5% glycerol, 75 mM potassium glutamate, 4 mM spermidine, 0.1 mM EDTA, 4 mM $MgCl_2$, 13 μM poly(dG-dC), 0.01% Nonidet P40, and 5 μg/mL bovine serum albumin. Reactions performed under the conditions of Petri et al. (*9*) contained 25 mM Bis-Tris, pH 7.4, 5 mM $MgCl_2$, 100 mM KCl, 2 mM DTT, and 1 μg/mL (3 μM) poly(dG-dC).

In Vitro BMH Cross-Linking Assay. In Figure 1, BMH cross-linking reactions were performed as previously described (*15*). Cross-linking was initiated by the addition of 0.1 mM BMH and 9% dimethyl sulfoxide. Mock reactions contained only dimethyl sulfoxide. Reactions were quenched with 10 μL of 2× protein sample buffer 90 s after addition of BMH. In Figure 3, reactions contained 10 mM Tris−acetate, pH 7.5, 10% glycerol, 1 mM $MgCl_2$, 60 mM potassium glutamate, 15 mM potassium chloride, 0.01% Nonidet-P40, and 110 nM bovine serum albumin.

GST Pull-Down Assay. GST-h180C was loaded onto glutathione resin and incubated at 300 nM under the final reaction conditions at 4 °C in a volume of 0.5 mL. Binding reactions at 4 °C were initiated upon addition of 10 nM yTBP, derived from a concentrated stock (2.5 μM). At various time points, the resin was collected by a brief centrifugation, and the supernate was discarded. No additional washes were performed on the resin. The resin was resuspended in protein sample buffer and loaded directly onto 10% polyacrylamide gels. Western blots were probed with yTBP antibodies. yTBP standards were used to ensure linearity of the quantitation. Autoradiographs were scanned by laser densitometry, and band intensities were quantitated using NIH Image software. Local background was subtracted, and the data were normalized to a globally fit value of 1.0. The plotted data were fit to the equation: reaction coordinate = $1 - e^{-kt}$, where k denotes the apparent first-order dissociation rate constant of the reaction.

DNA Binding Assays. The filter binding and electrophoretic mobility assays were performed as previously described (*13*, *16*). Radioactivity was quantitated using either a phosphorimager or a Betascope.

RESULTS

Cross-Linking of yTBP Dimers. We have employed the chemical cross-linker bis(maleimido)hexane (BMH) as one of many assays for detecting hTBP dimers (*14*, *15*). Under conditions where hTBP is mostly dimeric as measured by gel filtration and pull-down assays, only a small percentage of it becomes cross-linked into dimers, possibly due to other competing or nonproductive cross-linking reactions. Therefore, chemical cross-linking is not used to determine the absolute level of dimerization, but instead provides a relative assessment.

Because the crystallographic dimer interface resides within the conserved 180 C-terminal domain of TBP (180C), we wondered whether h180C and yTBP could form heterodimers as well as homodimers. In Figure 1A, h180C and full-length

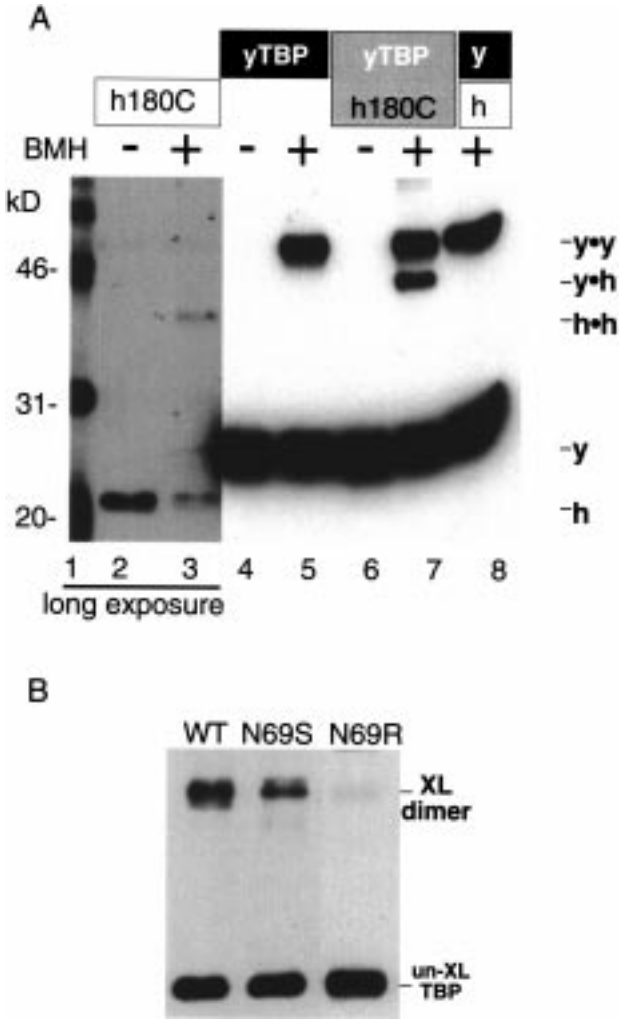

FIGURE 1: (A) h180C (2 μM) and yTBP (2 μM) were incubated either alone (lanes 2 and 3, and 4 and 5, respectively) or together (lanes 6 and 7), and then treated with BMH (+) or mock-treated (−). Quenched samples shown in lanes 3 and 5 were mixed together and loaded in lane 8. Samples were electrophoresed on an SDS−10% polyacrylamide gel and probed for yTBP by Western blotting (ECL). Molecular mass markers are in lane 1. The migration of cross-linked dimers is indicated by either 'y•y', 'y•h', or 'h•h', which correspond to yeast homodimers, yeast/human heterodimers, and human homodimers, respectively. Un-cross-linked hTBP and yTBP are denoted by 'y' and 'h', respectively. At these high TBP concentrations, a small amount of cross-linked tetramers were detected (not shown). (B) BMH cross-linking of wild-type and mutant yTBPs. 55 nM yTBP, that was either wild type (WT) or mutant (N69S or N69R), was incubated with BMH for 90 s at 30 °C. Reactions were quenched and electrophoresed on an SDS−10% polyacrylamide gel and probed for yTBP by Western blotting.

yTBP were treated with BMH either separately or after the two were mixed (lanes 2−7). h180C and yTBP each cross-linked into a single dimeric species of distinct mobility. Due to the poor cross-reactivity of yTBP antibodies with h180C, detection of h180C required a long exposure of the blot to film. When yTBP and h180C were mixed, a new species was detected having a mobility intermediate to yTBP and h180C. Both the mobility and the intensity of the band are consistent with the formation of a yTBP/h180C heterodimer, which indicates that the yeast and human TBP dimer interfaces are conserved. As a further control, to ensure that gel electrophoretic conditions did not artifactually cause heterodimer formation, individually cross-linked yTBP and h180C were mixed after quenching (lane 8). No heterodimer formation was observed.

Recently, we have characterized a number of mutations in the crystallographic yTBP dimer interface (*2*). The cross-linking of one set of mutants is presented in Figure 1B. At 55 nM, wild-type yTBP readily cross-linked into dimers, while N69S cross-linked with less efficiency and N69R was not detectably cross-linked. The arginine side chain being bulkier than serine is expected to be more disruptive. The data suggest that the dimers detected by BMH cross-linking are in a similar configuration as those detected in the crystalline lattice.

Kinetics of yTBP Dimer Dissociation. The primary assay that we used to measure the kinetics of dimer dissociation relies on the ability of purified wild-type or mutant polyhistidine-tagged yTBP to be retained on glutathione resin containing GST-180C (Figure 2A). GST-180C contains the core DNA binding and dimerization domain of hTBP fused to glutathione-*S*-transferase. We have previously documented the validity and specificity of various permutations of this assay in a number of studies using yeast and human TBPs (*2*, *5*, *14*). Kinetic profiles were identical whether core or full-length yTBP or hTBP was immobilized via a GST or polyhistidine tag, as long as the test protein lacked the same tag (data not shown). At various times after mixing the test yTBP with the resin, the free and bound yTBP were separated by a brief centrifugation. Bound yTBP was eluted, subjected to SDS−polyacrylamide gel electrophoresis, and detected by Western blotting.

In these exchange reactions, homodimers have the potential to compete with yTBP/GST-180C heterodimers. To ensure maximal exchange of input dimers to resin-bound heterodimers, as well as drive potentially unstable mutant heterodimers, a 30-fold molar excess of resin-bound GST-180C (300 nM) was employed. The kinetics of TBP retention on the resin are necessarily dictated by the rate of homodimer dissociation in solution. Otherwise, if heterodimer formation (the 'fast' step in Figure 2A) were slower than dimer dissociation (including resin-bound heterodimer dissociation), then no yTBP would be retained on the resin. Note that the kinetic rate constants derived from this assay provide a measure of homodimer stability in solution, and not stability with the resin-bound GST-180C. Mutations that moderately destabilize dimers are therefore expected to associate more rapidly with the resin. Mutants that do not appreciably dimerize are not expected to be retained on the resin.

Figure 2B illustrates the location of a few of the residues in the dimer interface that we have mutated and measured the kinetics of dimer dissociation. At some sites, more than one mutation was generated. As shown in Figure 2C,D, 10 nM yTBP was retained on the resin with fairly slow kinetics ($t_{1/2}$ = 23 min). Higher concentrations of GST-180C did not alter the kinetics (data not shown), which indicates that the kinetics reflect the intrinsic dissociation of yTBP dimers. The kinetics of yTBP dimer dissociation were of similar magnitude to that previously observed with hTBP, performed under similar conditions (*5*).

Several mutants (N69S, V161E, S184R, E186Q, and L189R) were retained on the resin with faster kinetics ($t_{1/2}$ ranging from 6 to 11 min), indicating that these residues lie along the dimer interface and mutating them destabilizes the dimer. When a bulkier charged substitution (arginine) is

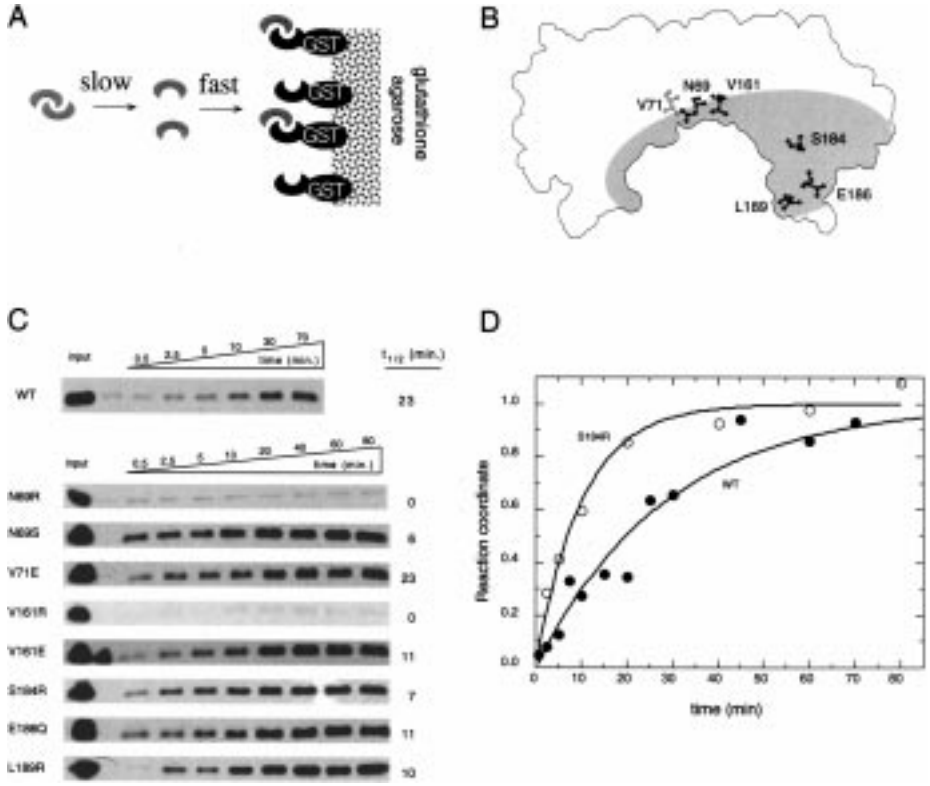

FIGURE 2: (A) Schematic of the pull-down assay. (B) An outline of yTBP(180C), indicating the location of mutated residues. The shaded area represents the approximate location of the dimer interface. (C) Western blot data showing the dimer dissociation kinetics of 10 nM yTBP at 4 °C in the presence of 300 nM resin-bound GST-h180C. The $t_{1/2}$ of dimer dissociation was determined from curve-fitting of plotted data, as exemplified in panel D. Standard errors were typically between 10 and 20%. (D) Representative plots of normalized data obtained from panel C and other data not shown. The dimer dissociation rate constant for wild-type TBP in this experiment was $(5.8 \pm 0.5) \times 10^{-4}$ s^{-1}.

placed at either N69 or V161, yTBP was not retained, indicating that these severe mutations prevent dimerization. V71 lies just outside of the 4 Å crystallographic dimer interface, and a mutation to aspartate at this position did not noticeably affect the stability of the dimer. In general, the kinetic profiles of the wild-type and mutant yTBPs can be reconciled by the dimer crystal structure, which indicates that (1) the assay provides a valid and specific measure of dimer stability, (2) dimers are prevalent at nanomolar concentrations as previously determined for hTBP (*14*), and (3) the dimer interface in solution is similar to that in the crystal structure. These findings do not exclude the possibility that higher order structures (e.g., dimers of dimers) might be present. Low amounts of higher order yTBP complexes are detected in the BMH cross-linking assay, particularly at micromolar concentrations (not shown). Their abundance cannot be ascertained using this assay, in that higher order structures might cross-link with different efficiencies than dimers.

yTBP Dimer Dissociation Is Rate-Limiting for DNA Binding. The slow dissociation of yTBP dimers implies that dimer dissociation will dictate the kinetics of DNA binding, as was previously observed with hTBP (*5*). To address this possibility, 55 nM yTBP was challenged with excess (110 nM) TATA or mutant TATA oligonucleotide at 22 °C. At various times, the relative levels of yTBP dimers remaining were determined using the BMH cross-linking assay. As shown in Figure 3A,B, dimers dissociated slowly in the presence of TATA DNA, but not in the presence of mutant TATA. The $t_{1/2}$ of dimer dissociation was approximately 10 min, which is of similar magnitude as the rate of dimer dissociation determined by the pull-down assay (~23 min).

Next we examined the kinetics of DNA binding directly using the electrophoretic mobility shift assay. We employed 100 nM yTBP, which is expected to be present as a mixed population of monomers and dimers, and excess (300 nM) TATA DNA to examine the binding of the entire yTBP population. As shown in Figure 3C, we see a rapid 'burst' of monomer binding within the first minute which is not resolved in this assay. The burst is followed by a slow phase corresponding to a slow dissociation of dimers. The biphasic nature of this curve is characteristic of two active populations of TBP present, and has been described in detail for hTBP elsewhere (*5*). Taken together, the data suggest that the rate of yTBP dimer dissociation dictates the kinetics of DNA binding.

Inactivation of TBP. A previous study on yTBP has demonstrated rapid binding kinetics and a linear k_{obs} relationship with [yTBP] (*9*), which is apparently inconsistent with the presence of dimers. To address this discrepancy, we performed additional kinetic analyses of yTBP binding to TATA DNA. To rule out differences in protein preparations, assays, and operator error, our first step was to reproduce the same kinetic behavior under the previously defined conditions (25 mM Bis-Tris, 5 mM $MgCl_2$, 100 mM KCl, 2 mM DTT, 1 μg/mL poly(dG-dC), pH 7.4). As shown in Figure 4A, at 50 nM yTBP and <1 nM TATA DNA at 22 °C, the kinetics proceeded rapidly, having a $t_{1/2} = <1$ min. The apparent bimolecular association rate constant k_a for this reaction was 2.6×10^5 M^{-1} s^{-1}, which is of similar

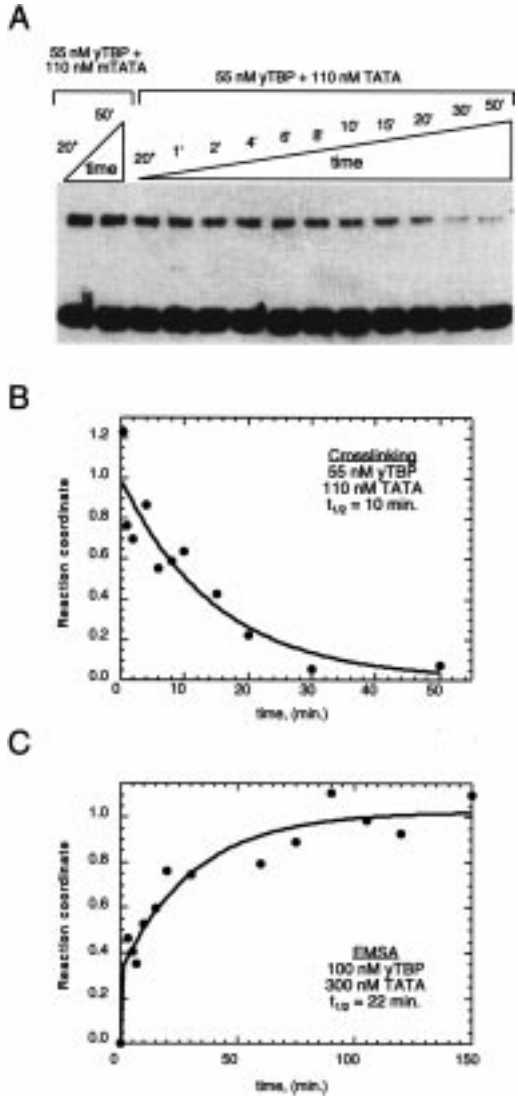

FIGURE 3: Kinetics of dimer dissociation in the presence of TATA DNA. (A) 55 nM yTBP was incubated with 110 nM of either mutant TATA (lanes 1 and 2) or TATA (lanes 3−13) at 22 °C for the indicated time under the conditions described under Materials and Methods. BMH (1 mM) was then added for 15 s at 30 °C, and then quenched with 2× protein sample buffer. Cross-linked yTBP dimers and un-cross-linked yTBP were separated by SDS−polyacrylamide gel electrophoresis, and yTBP was analyzed by Western blotting. (B) The fractional change in dimer intensity (reaction coordinate) from panel A was plotted as a function of time and fit to the equation: reaction coordinate $= e^{-kt}$, where k is the pseudo-first order observed rate constant, which was determined to be $(1.1 \pm 0.2) \times 10^{-3}$ s^{-1}. (C) Kinetics of yTBP (100 nM) binding to excess TATA DNA (300 nM) as measured by the electrophoretic mobility shift assay. Radioactivity present in the shifted TBP/TATA complex was quantitated, normalized to 1.0, and plotted as a function of time. Data were fit to the double exponential: reaction coordinate $= m1(1 - e^{-m2t}) + m3(1 - e^{-m4t})$, where $m1$, $m2$, $m3$, and $m4$ are constants evaluated by the Kaleidagraph fitting program. To obtain k_{obs} for the slow phase of the reaction, the data (excluding the zero point) were fit to a single exponential. k_{obs} was determined to be $(5 \pm 2) \times 10^{-4}$ s^{-1}. A reaction in which yTBP was omitted was used as the zero time point.

magnitude to that previously reported under these conditions (2.1×10^5 M^{-1} s^{-1}) (*9*).

Surprisingly, though, prolonged (∼1 h) preincubation of yTBP in the absence of DNA, as was previously done (*9*), caused a 4−5-fold reduction in the overall yield of the TBP/TATA complex (Figure 4A). Note that the yield reduction occurred despite the [yTBP] being in vast excess over [TATA], and well above the reported K_D (∼3 nM) under these conditions. We suspect that under these conditions, preincubation of yTBP in the absence of TATA DNA might lead to inactivation of yTBP's DNA binding activity.

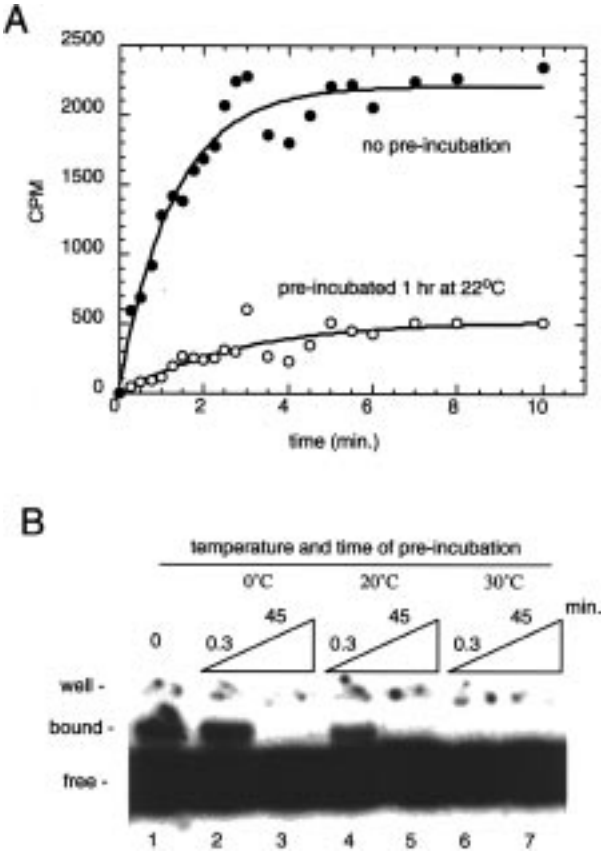

FIGURE 4: DNA binding under the conditions of Petri et al. (*9*). (A) Reactions contained 50 nM yTBP and <1 nM radiolabeled TATA DNA. (●) Binding reactions at 22 °C were initiated upon addition of yTBP derived from a concentrated stock stored on ice. (○) yTBP was incubated under the final binding conditions for 1 h at 22 °C; then TATA DNA was added to initiate the reaction. At various time points, DNA binding was detected using a filter binding assay. 'CPM' denotes the amount of radioactivity present on the filter after background subtraction. Data were fit to the equation: CPM $= m1(1 - e^{-m2t})$. $m2$ (or k_{obs}) for each reaction was (●) $(2.7 \pm 0.3) \times 10^5$ M^{-1} s^{-1} and (○) $(1.2 \pm 0.3) \times 10^5$ M^{-1} s^{-1}. (B) Same as in panel A, except that 2 nM TATA oligo was used to initiate DNA binding. Preincubation times and temperatures of yTBP under the final binding conditions (in the absence of TATA DNA) are indicated. Reactions were chilled on ice and stabilized with 5% glycerol and 0.01% Nonidet P40 prior to DNA binding at 0 °C. DNA binding was assayed by the electrophoretic mobility shift assay. To minimize potential dissociation of yTBP in the gel (*8*), the electrophoresis time was reduced from the standard 60−600 min (*8*, *17*) to 15 min.

To address the possibility that yTBP might become largely inactivated while preincubated in the absence of DNA, 100 nM yTBP was preincubated as described above, for either 0, 0.3, or 45 min at either 0, 20, or 30 °C. At the end of the incubation period, samples were placed on ice, and 5% glycerol and 0.01% Nonidet P40 were added to enhance the stability of yTBP. Incubations were continued on ice until all reactions had been preincubated for a total of 45 min. Radiolabeled TATA DNA (∼2 nM) was then added, and incubations on ice were continued for 75 min. TBP/TATA

complexes were then separated from free probe using the electrophoretic mobility shift assay.

There are several reasons why this strategy was chosen. First, to minimize any potential inactivation during the TATA binding stage, binding reactions were performed at 0 °C, where free TBP is more stable. To measure the DNA binding activity of the entire TBP population, our initial attempts included excess TATA over TBP. However, under these conditions we could detect very little binding of TBP to TATA. Because the data in Figure 4A suggested that much of the yTBP was becoming inactivated, we reduced the TATA concentration to 2 nM to achieve a greater signal-to-noise ratio, which is still ~1000-fold greater than that used previously (*9*). We also found that adding glycerol and Nonidet P40 prevented further inactivation at 0 °C.

As shown in Figure 4B (and data not shown), the vast majority of yTBP's DNA binding activity was lost after only 0.3 min of incubation at 30 °C (compare lanes 1 and 6). At lower temperatures, the DNA binding activity was slightly more stable (lanes 2 and 4). However, after 45 min, DNA binding activity was lost at all temperatures tested, including 0 °C (lanes 3, 5, and 7). Together, the data in Figure 4 reveal that preincubation of yTBP in the absence of TATA DNA, under conditions previously used to define TBP/TATA binding kinetics (*9*), rapidly inactivates the protein.

In an effort to further characterize the instability of TBP's DNA binding activity in the absence of DNA, we focused on human TBP, whose self-association and DNA binding activity we have extensively characterized, and found to be indistinguishable from yTBP. Our reactions include 20 mM Tris−acetate, pH 7.5, 5% glycerol, 75 mM potassium glutamate, 4 mM spermidine, 4 mM $MgCl_2$, 13 μM poly(dG-dC), 0.01% Nonidet P40, and 5 μg/mL bovine serum albumin. These conditions help stabilize TBP, particularly at 0 °C, where we detect no loss of DNA binding activity for incubation periods as long as 6 h (data not shown). Various concentrations of hTBP (10, 30, 100, and 200 nM) were incubated under these conditions at 30 °C in the absence of TATA DNA. At various time points, samples were placed on ice and diluted to 10 nM. Excess TATA DNA (30 nM) was then added, and incubations on ice were continued for 90 min. TBP/TATA complex formation was measured with the nitrocellulose filter binding assay. As shown in Figure 5A, hTBP was remarkably unstable at all concentrations tested ($t_{1/2}$ ranging from 6 to 26 min), but appeared to be more stable at higher concentrations.

When the observed inactivation rate constants ($k_{inact.}$) were plotted as a function of [TBP] (Figure 5B), a significant concentration dependence was observed, which appeared to vary inversely with the square root of the [TBP]. Apparently, at least over a concentration range of 10−200 nM, TBP self-association stabilizes TBP against inactivation.

DISCUSSION

The recruitment of TBP to a promoter is an important rate-limiting step in gene expression in vivo. In the absence of an activator, TBP is unable to access promoter DNA efficiently. Because TBP can bind TATA DNA with high affinity in vitro, it appears that factors must block TATA and/or TBP in vivo to prevent association. Using a combined biochemical and genetic approach, we have recently found that yTBP dimerizes through its conserved carboxyl-terminal domain in accordance with its crystallographic structure (*2*). Moreover, yTBP dimerization appears to prevent unregulated gene expression and its own degradation in vivo. These findings with yTBP confirm our previous findings with human TBP dimers (*5*, *14*, *15*), which employed four distinct assays (pull-down, cross-linking, gel filtration, and DNA binding kinetics) to demonstrate dimerization.

Because TBP dimerization plays a central inhibitory role in regulating transcription complex assembly at least in yeast, an understanding of the dynamics of yTBP dimer dissociation is critical to defining rate-limiting steps in gene expression. Using a pull-down-based assay, we find that yTBP dimers dissociate slowly, having a $t_{1/2}$ of approximately 20 min under our in vitro conditions. Severe mutations in the crystallographic dimer interface prevent yTBP dimerization, and more mild mutations accelerate the kinetics of dissociation. These mutants provide important specificity controls for both the assay and the determined kinetic rate constants. A slow dissociation of dimers has the potential to dictate the kinetics of DNA binding. This possibility was addressed in two ways. BMH chemical cross-linking was used to measure the loss of dimers upon addition of TATA DNA. An electrophoretic mobility shift assay was used to directly measure the binding of TBP to TATA DNA. Both assays produced slow kinetic profiles of similar magnitude as those of the dimer dissociation kinetics measured in the absence of DNA. Taken together, these data indicate that the rate of yTBP dimer dissociation, like hTBP, is kinetically rate-limiting for DNA binding in vitro.

When kinetic analyses are performed in the presence of a large (10^1-10^5) molar excess of TBP over DNA, rapid kinetics are observed (*5*, *6*, *8*, *10*). This rapid binding might correspond to the small fraction of TBP monomers present in a typical dimer/monomer equilibrium, which is nevertheless in excess of the [TATA]. Such studies have revealed that the association of TBP monomers with DNA is limited by the simultaneous binding and bending of the TATA DNA. Monomer binding is therefore second-order and not limited by a slow isomerization of the TBP/TATA complex. None of the data presented here or elsewhere discount that notion. Instead, TBP appears to have at least two distinct mechanism for preventing promiscuous binding to DNA: dimerization, and a need to simultaneously bind and bend TATA DNA. A third potential mechanism, instability, is described below.

Apparent Discrepancy with Kinetic Studies That Fail To Detect yTBP Dimers. A number of studies have not detected yTBP dimers (*8*−*11*). In one study (*9*), an apparently linear response of k_{obs} to total [TBP] argues against the presence of dimers. k_{obs} is defined as the pseudo-first-order rate constant for the decay of free DNA (D) into a TBP/DNA (TD) complex, at a particular excess *total* [TBP] (Figure 6A). Because [TBP] ≫ [DNA], the unbound [TBP] does not appreciably change over the course of the reaction, and so the reaction is adequately described with a first-order rate constant. The assumption inherent in k_{obs} is that the total [TBP] is equivalent to the monomer (T) concentration that is active for DNA binding. If this is true, then k_{obs} will vary linearly with total [TBP]. If this assumption is not true, then k_{obs} will be some function of the various equilibria linked to active monomers.

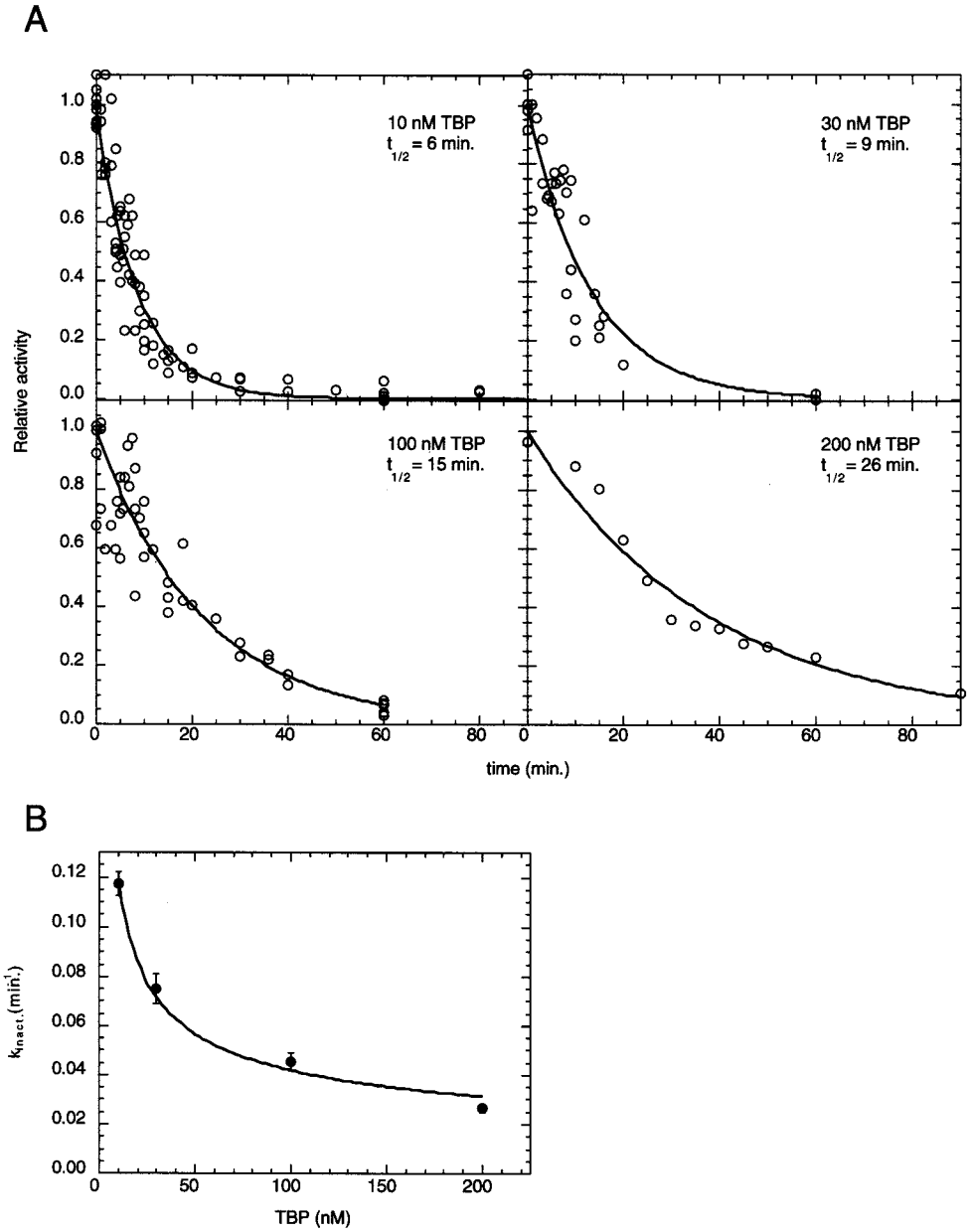

FIGURE 5: Instability of hTBP DNA binding activity. (A) hTBP, at the concentrations indicated in each panel, was preincubated at 30 °C in the absence of TATA DNA for the time periods indicated along the *x*-axis. TBP was then chilled on ice, diluted to 10 nM, and incubated with 30 nM radiolabeled TATA DNA for 90 min at 0 °C. All data were normalized to globally fitted value of 1.0, which represents the average binding in the absence of preincubation. Data were fit to the equation: relative activity $= e^{-kt}$, where k is the observed inactivation rate constant. Because all DNA binding reactions were performed under pseudo-first-order conditions of excess TATA DNA (30 nM), and well above the apparent K_D (0.5 nM), nearly all active TBP is expected to be driven into a TBP/TATA complex. (B) The observed inactivation rate constant ($k_{inact.}$) determined in panel A was plotted as a function of total hTBP concentration. Data were fit using Kaleidagraph software to the equation $k_{inact.} = (m1/[TBP]^{1/2}) + m2$, where $m1$ and $m2$ are computer-fitted constants ($m1 = 0.38 \pm 0.03$; $m2 = 0.006 \pm 0.005$).

If dimers (TT in Figure 6A) are prevalent, then k_{obs} is expected to vary directly with the square root of the total [TBP]. In Figure 6B, the previously reported linear response is illustrated as a dashed line. If the same data are fit to a kinetic mechanism which invokes TBP dimerization in competition with DNA binding, the solid curve is obtained. Within the error limits imposed by data collection over this concentration range, both curves might accommodate the data.

Nevertheless, we undertook a study to identify other potential linked equilibria that might contribute to k_{obs}. We found that TBP's DNA binding activity was extremely labile in the absence of DNA under the conditions employed by Petri et al. More detailed analyses with hTBP under somewhat more stable conditions revealed that the rate of TBP inactivation was concentration-dependent. TBP stability appeared to increase with the square root of [TBP], tested in the range of 10−200 nM. The apparent square root dependence suggested that dimerization might stabilize TBP against inactivation. Alternatively, the data do not exclude the possibility that tetramers stabilize dimers against inactivation. Regardless, a second inactivation equilibrium appears to be linked to free TBP ($T_{inactive}$ in Figure 6A). Because TBP inactivation appears to be irreversible, the net effect of preincubating a fixed total [TBP] in the absence of DNA under standard in vitro conditions is to swap one 'inactive'

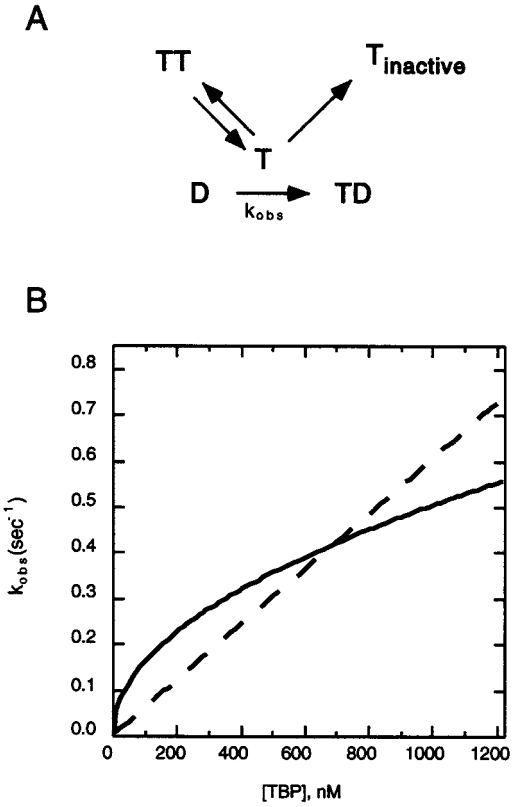

FIGURE 6: Relationship between k_{obs} and [TBP] will vary depending upon the mechanism. (A) A possible mechanism describing the competing linked equilibria monomeric TBP faces under pseudo-first-order conditions of excess monomeric TBP (T). The competing linked equilibria include dimerization (TT) and inactivation ($T_{inactive}$). k_{obs} describes the pseudo-first-order conversion of TATA DNA (D) to a stable TBP/TATA complex (TD). For a particular total [TBP], the experimentally determined k_{obs} is dependent on the ratios of TT, T, and $T_{inactive}$. (B) The dashed line represents a linear fit to the data of Petri et al. (*9*, Figure 6, ML 30 °C). The same data were fit using Kaleidagraph software to the equation $k_{obs} = m1[TBP]^{1/2}$ (solid curve), where $m1$ is a computer-fitted constant. An identical curve was obtained using KINSIM software, inputting the previously described dimer mechanism (*5*) and the kinetic parameters of Petri et al. (1998).

form of TBP (the reversible dimer) with another. In the process, the active monomer concentration stays relatively constant (steady-state). Thus, under conditions where dimers are initially prevalent, extensive inactivation of TBP might have only small effects on k_{obs}, determined in the presence of excess TBP over DNA. At lower [TBP], where monomers are more prevalent, the more rapid rate of TBP inactivation would lead to greater drops in k_{obs}. This, in effect, might flatten out the lower end of the theoretical curve in Figure 6B, making the overall relationship between k_{obs} and [TBP] appear more linear.

An alternative kinetic approach to evaluating the presence of linked equilibria is to perform the DNA binding kinetics in the presence of excess TATA DNA. If no linked equilibria exist, and the total [TBP] is equivalent to the total active [monomer], then the bimolecular association rate constant k_a ought to be similar to that obtained in the presence of excess TBP. To the contrary, two studies other than our own, that were performed in the presence of excess DNA, have reported a k_a that was 10−45-fold lower than that obtained in the presence of excess protein (*6*, *17*). If dimer dissociation is rate-limiting for the binding of a substantial portion of the total TBP population, then a biphasic binding curve should be obtained (*5*). Such a biphasic response is observed for yTBP (Figure 3C). The burst phase reflects the binding of monomers and can be used to derive k_a. If the slow phase is used to evaluate k_a, a significantly lower value will be obtained.

Apparent Discrepancy with Self-Association Studies in the Absence of DNA. TBP inactivation might also explain the apparent discrepancy of the dimer model with analytical ultracentrifugation studies on yTBP. Daugherty et al. (*11*) reported that yTBP undergoes a highly cooperative monomer to tetramer (and octamer) equilibria, having a K_D in the micromolar range. The conditions used in that study are similar to that of Petri et al. (*9*), which we have found to rapidly inactivate yTBP, particularly in the lower concentration ranges. It is possible that tetramer and octamer formation of yTBP in the micromolar range 'locks' yTBP into a conformation that prevents it from becoming inactivated, although it is not clear whether tetramers and octamers represent an active or an inactive state. At lower concentrations, where higher order structures are expected to be less prevalent, the rapid inactivation of yTBP monomers upon long (∼12 h) incubations of TBP in the absence of TATA DNA would in effect drain the dimer population as well. This might account for the inability to detect dimers, and the appearance of a monomer−tetramer equilibrium.

Perez-Howard et al. (*6*) have reported the presence of multimeric species of yTBP using tryptophan fluorescence spectroscopy. Interestingly, they report that variable handling of yTBP (repeated freeze/thaws etc.) can induce monomerization and accelerated DNA binding kinetics. This might account for why reported k_a values under identical conditions vary by as much as 10-fold (*9*, *10*). Perez-Howard et al. (*6*) also find that at 30 °C yTBP appears to initiate the first step in a two-stage unfolding process. This first step might include monomerization followed by inactivation.

Implications of Self-Association. It is clear that TBP monomers bind TATA DNA rapidly and with high affinity. However, TBP has relatively low specificity for TATA. TBP's ability to discriminate a random site from a strong TATA box is about 1000-fold lower than that of a typical sequence-specific major groove DNA binding protein to its cognate site (*13*). In vitro, whether TBP is bound to TATA or to a nonspecific site, it can nucleate the assembly of a functional transcription complex (*13*). Therefore, if TBP monomer's DNA binding activity is left unchecked in the cell it would have the potential to initiate chromosomal transcription randomly. It would also initiate transcription at TATA-containing promoters in an unregulated manner. Promiscuous DNA binding might be kept in check via a number of mechanisms including DNA-bound repressors (chromatin), TBP repressors, TBP dimerization, and a need to recognize distorted DNA. In addition to these mechanisms, TBP might be designed such that the active DNA binding conformation of isolated monomers is unstable. In the absence of the stabilizing effect caused by DNA binding or dimerization, TBP's DNA binding activity might be rapidly lost in vivo. Consistent with this notion, molecular dynamics computational simulations predict an extraordinary level of conformational flexibility of TBP monomers, including a near-collapse of its DNA binding surface (*18*). From a physiological perspective, monomer instability is consistent

with the finding that genetically forced TBP monomers are degraded very rapidly in vivo (*2*).

REFERENCES

1. Hernandez, N. (1993) *Genes Dev. 7*, 1291−1308.
2. Jackson-Fisher, A. J., Chitikila, C., Mitra, M., and Pugh, B. F. (1999) *Mol. Cell 3*, 717−727.
3. Kim, J. L., Nikolov, D. B., and Burley, S. K. (1993) *Nature 365*, 520−527.
4. Nikolov, D. B., Hu, S. H., Lin, J., Gasch, A., Hoffmann, A., Horikoshi, M., Chua, N. H., Roeder, R. G., and Burley, S. K. (1992) *Nature 360*, 40−46.
5. Coleman, R. A., and Pugh, B. F. (1997) *Proc. Natl. Acad. Sci. U.S.A. 94*, 7221−7226.
6. Perez-Howard, G. M., Weil, P. A., and Beechem, J. M. (1995) *Biochemistry 34*, 8005−8017.
7. Kato, K., Makino, Y., Kishimoto, T., Yamauchi, J., Kato, S., Muramatsu, M., and Tamura, T. (1994) *Nucleic Acids Res. 22*, 1179−1185.
8. Hoopes, B. C., LeBlanc, J. F., and Hawley, D. K. (1992) *J. Biol. Chem. 267*, 11539−11547.
9. Petri, V., Hsieh, M., Jamison, E., and Brenowitz, M. (1998) *Biochemistry 37*, 15842−15849.
10. Parkhurst, K. M., Brenowitz, M., and Parkhurst, L. J. (1996) *Biochemistry 35*, 7459−7465.
11. Daugherty, M. A., Brenowitz, M., and Fried, M. G. (1999) *J. Mol. Biol. 285*, 1389−1399.
12. Nakajima, N., Horikoshi, M., and Roeder, R. G. (1988) *Mol. Cell. Biol. 8*, 4028−4040.
13. Coleman, R. A., and Pugh, B. F. (1995) *J. Biol. Chem. 270*, 13850−13859.
14. Coleman, R. A., Taggart, A. K., Benjamin, L. R., and Pugh, B. F. (1995) *J. Biol. Chem. 270*, 13842−13849.
15. Taggart, A. K., and Pugh, B. F. (1996) *Science 272*, 1331−1333.
16. Chicca, J. J., Auble, D. T., and Pugh, B. F. (1998) *Mol. Cell. Biol. 18*, 1701−1710.
17. Kuddus, R., and Schmidt, M. C. (1993) *Nucleic Acids Res. 21*, 1789−1796.
18. Miaskiewicz, K., and Ornstein, R. L. (1996) *J. Biomol. Struct. Dyn. 13*, 593−600.

BI990911P